Top-down alteration of functional connectivity within the sensorimotor network in focal dystonia

Giovanni Battistella, PhD, and Kristina Simonyan, MD, PhD, Dr.med

Neurology® 2019;92:e1843-e1851. doi:10.1212/WNL.0000000000007317

Correspondence
Dr. Simonyan
kristina_simonyan@
meei.harvard.edu

Abstract

Objectives

To determine the directionality of regional interactions and influences of one region on another within the functionally abnormal sensorimotor network in isolated focal dystonia.

Methods

A total of 40 patients with spasmodic dysphonia with and without dystonic tremor of voice and 35 healthy controls participated in the study. Independent component analysis (ICA) of resting-state fMRI was used to identify 4 abnormally coupled brain regions within the functional sensorimotor network in all patients compared to controls. Follow-up spectral dynamic causal modeling (DCM) estimated regional effective connectivity between patients and controls and between patients with spasmodic dysphonia with and without dystonic tremor of voice to expand the understanding of symptomatologic variability associated with this disorder.

Results

ICA found abnormally reduced functional connectivity of the left inferior parietal cortex, putamen, and bilateral premotor cortex in all patients compared to controls, pointing to a largely overlapping pathophysiology of focal dystonia and dystonic tremor. DCM determined that the disruption of the sensorimotor network was both top-down, involving hyperexcitable parieto-putaminal influence, and interhemispheric, involving right-to-left hyperexcitable premotor coupling in all patients compared to controls. These regional alterations were associated with their abnormal self-inhibitory function when comparing patients with spasmodic dysphonia patients with and without dystonic tremor of voice.
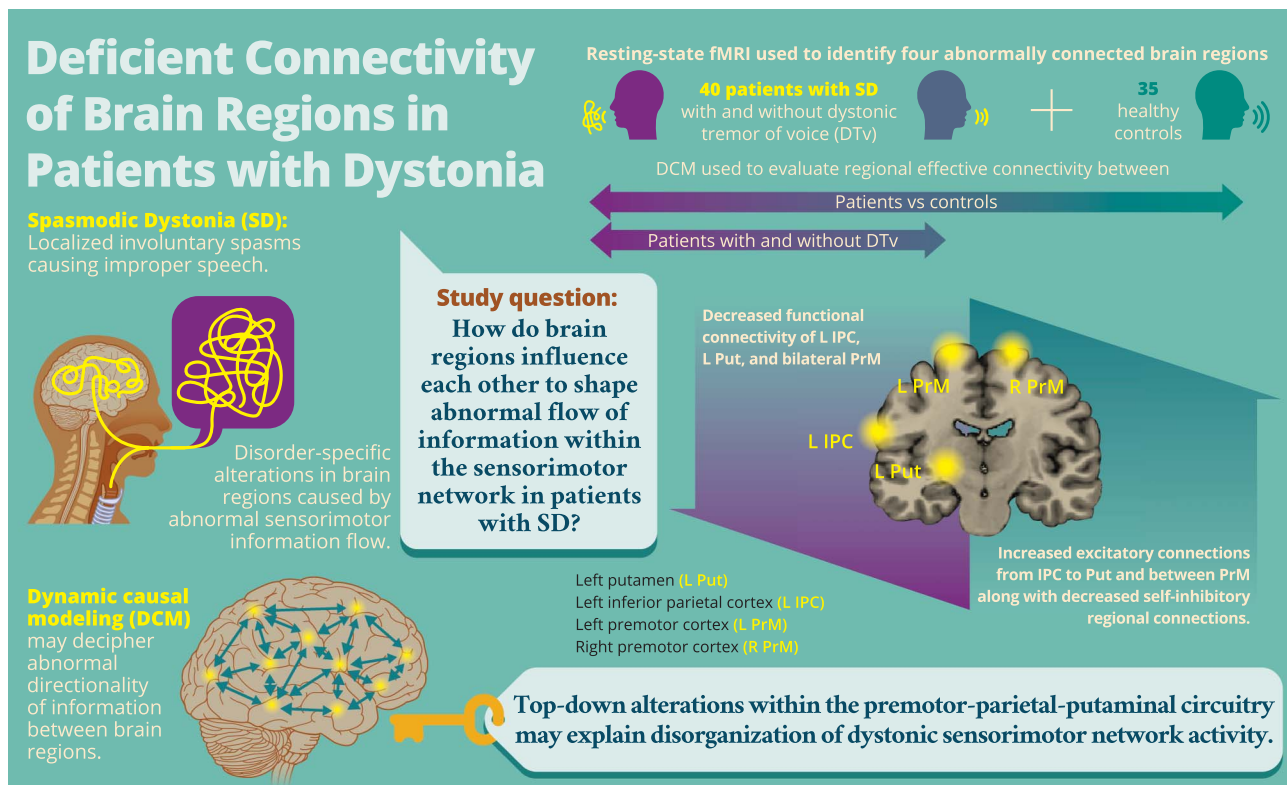
Conclusions

Abnormal hyperexcitability of premotor-parietal-putaminal circuitry may be explained by altered information transfer between these regions due to underlying deficient connectivity. Identification of brain regions involved in processing of sensorimotor information in preparation for movement execution suggests that complex network disruption is staged well before the dystonic behavior is produced by the primary motor cortex.

From the Memory and Aging Center (G.B.), Department of Neurology, University of California San Francisco; Department of Otolaryngology (K.S.), Massachusetts Eye and Ear; Department of Neurology (K.S.), Massachusetts General Hospital (K.S.); and Harvard Medical School (K.S.), Boston, MA.

Glossary

DCM = dynamic causal modeling; **DTv** = dystonic tremor of voice; **GLM** = general linear model; **ICA** = independent component analysis; **IPC** = inferior parietal cortex; **MPRAGE** = magnetization-prepared rapid acquisition with gradient echo; **MSN** = medium spiny neuron; **PEB** = parametric empirical Bayes; **PP** = posterior probability; **ROI** = region of interest; **SD** = spasmodic dystonia; **WM** = white matter.

Deficient Connectivity of Brain Regions in Patients with Dystonia

Resting-state fMRI used to identify four abnormally connected brain regions

40 patients with SD with and without dystonic tremor of voice (DTv)

35 healthy controls

DCM used to evaluate regional effective connectivity between

Patients vs controls

Patients with and without DTv

Spasmodic Dystonia (SD): Localized involuntary spasms causing improper speech.

Disorder-specific alterations in brain regions caused by abnormal sensorimotor information flow.

Study question: How do brain regions influence each other to shape abnormal flow of information within the sensorimotor network in patients with SD?

Dynamic causal modeling (DCM) may decipher abnormal directionality of information between brain regions.

Decreased functional connectivity of L IPC, L Put, and bilateral PrM

L PrM   R PrM   L IPC   L Put

Increased excitatory connections from IPC to Put and between PrM along with decreased self-inhibitory regional connections.

Left putamen (L Put)
Left inferior parietal cortex (L IPC)
Left premotor cortex (L PrM)
Right premotor cortex (R PrM)

Top-down alterations within the premotor-parietal-putaminal circuitry may explain disorganization of dystonic sensorimotor network activity.

NPub.org/935320   DOI: 10.1212/WNL.0000000000007317

Neurology®

Copyright © 2019 American Academy of Neurology

Dystonia is a debilitating movement disorder of unclear causative mechanisms. Recent neuroimaging studies demonstrated disorder-specific alterations in brain regions responsible for sensorimotor control, aberrant excitation and inhibition of the basal ganglia circuitry, and abnormal integration of basal ganglia, thalamus, and cerebellum with primary sensorimotor and inferior parietal regions within the dystonic functional connectome.[1–11] However, it remains unknown how abnormal information flows within the dystonic network, which hinders our understanding of the full spectrum of pathophysiologic interactions in this disorder, while the differentiation between its causative and compensatory neural changes remains elusive.

To examine the directionality of abnormal influences of one region on another, we used spectral dynamic causal modeling (DCM) of resting-state fMRI in patients with spasmodic dystonia (SD), a laryngeal form of isolated focal task-specific dystonia, compared to healthy controls. We built DCM analysis on the basis of the results of independent component analysis (ICA) that identified abnormally coupled brain regions within the functional sensorimotor network in patients with SD compared to healthy controls. We further examined effective connectivity in patients with SD with and without dystonic tremor of voice (DTv) to expand the understanding of broader symptomatologic variability associated with dystonia. We hypothesized the presence of a top-down flow of abnormal information from sensorimotor cortical regions to basal ganglia where aberrant excitation and inhibition contribute to abnormal striato-cortical feedback loop, collectively sustaining the continuous cycle of pathologic dystonic activity.

Methods

Participants

Forty patients (10 male/30 female, mean age 53.9 ± 9.5 years) and 35 healthy controls (13 male/22 female, mean age 50.4 ± 10.6 years) participated in the study (table 1). Twenty patients were diagnosed with isolated focal SD (7 male/13 female, mean age 52.2 ± 7.3 years), whereas 20 patients had

Table 1 Demographic characteristics of the enrolled participants

	Healthy controls	Spasmodic dysphonia	Spasmodic dysphonia and dystonic voice tremor
No.	35	20	20
Male/female, n	13/22	7/13	3/17
Age, mean ± SD, y	50.4 ± 10.6	52.2 ± 7.3	55.5 ± 11.2
Language		Monolingual native English	
Handedness		Right	
Genetic status		Negative for DYT1, DYT6, DYT4, and DYT25 gene mutations	

SD combined with DTv (3 male/17 female, age 55.5 ± 11.2 years). There were no significant differences in age and sex between both patient and healthy control groups and between patients with SD and those with SD/DTv (all $p \geq 0.14$). All participants were right-handed and native English speakers, and none had any history of psychiatric or neurologic problems (except for SD and DTv in the patient groups). Diagnosis was established on the basis of a combination of perceptual voice evaluation and laryngological and neurologic examinations. All patients were fully symptomatic at the time of study participation; those who received botulinum toxin injections participated at least 3 months after the last treatment when fully symptomatic. Neuroradiologic evaluation showed normal brain structure in all participants without any gross abnormalities. None of patients were carriers of *TOR1A* (DYT1), *THAP1* (DYT6), *TUBB4A* (DYT4), or *GNAL* (DYT25) mutations as confirmed by genetic screening.

The Institutional Review Board of the Massachusetts Eye and Ear approved the study, and all participants provided written informed consent for study participation.

MRI acquisition protocol
All images were acquired on a Philips 3T scanner (Best, the Netherlands) with an 8-channel head coil. A sagittal T1-weighted gradient-echo sequence (magnetization-prepared rapid acquisition with gradient echo [MPRAGE]) was collected as part of the protocol for the registration of functional images. The MPRAGE image consisted of 172 contiguous slices, 1-mm isotropic voxel, repetition time of 2,300 ms, echo time of 2.98 ms, and field of view of 210 mm.

Resting-state fMRI data were obtained with a single-shot echo-planar imaging gradient echo sequence (repetition time 2,000 ms, echo time 30 ms, flip angle 90°, field of view 240 mm, voxel size 3 × 3 mm, 33 slices 3.5-mm thick covering the whole brain, 150 volumes). All participants were instructed to keep their eyes closed without falling asleep or thinking of anything in particular during image acquisition; the light and ambient noise were minimized in the scanner room. Cushioning of the participant's head with padding inside the coil minimized the head movements.

Data analysis
We performed resting-state fMRI data processing and DCM analyses using a combination of FSL, AFNI, and SPM software following the analytic pipeline shown in figure 1. The main steps included preprocessing of resting-state fMRI data; ICA to determine functional connectivity of sensorimotor network and to identify abnormal regions of interest (ROIs) as an input to DCM; extraction of ROI time series using a general linear model (GLM) based on discrete cosine transformation of the fMRI signal across resting-state frequency characteristics; definition and estimation of DCM to examine effective connectivity; and between-group group analyses using parametric empirical Bayes (PEB), a novel approach that permits group comparisons across model parameters using both posterior expectations and posterior uncertainties of the model.[12]

Data processing and identification of ROIs
We performed preprocessing of resting-state fMRI data and ICA using a combination of FSL and AFNI software, as previously described.[4,5] After removal of the first 4 volumes of resting-state data for magnetization stabilization, each brain volume was motion corrected, masked to exclude voxels outside of the brain, and high-pass filtered with a cutoff frequency of 0.01 Hz. Functional images were registered to the individual MPRAGE image with the use of 6-parameter rigid transformation, which was registered to the AFNI standard Talairach space with an affine algorithm. The 6 motion parameters (3 translation and 3 rotation) were calculated during realignment. The normalization was optimized with a nonlinear algorithm in AFNI software. Resultant images were smoothed with a Gaussian kernel full width at half-maximum of 5 mm, and the mean-based intensity was normalized by scaling all volumes by a factor of 1,000. These images were then used as an input for group ICA.

Nuisance removal
To control for motion and physiologic noise effects, we regressed individual 4-dimensional time series using 8 parameters: 2 for white matter (WM) and CSF mean signals and 6 for possible motion. We extracted WM and CSF

covariates by automatically segmenting the individual MPRAGE in the individual native space into gray matter, WM, and CSF using the unified segmentation algorithm[13] in SPM8 software. WM and CSF maps were thresholded at 90% of tissue probability, and all voxels in the masks were averaged across time series to extract nuisance regressors.
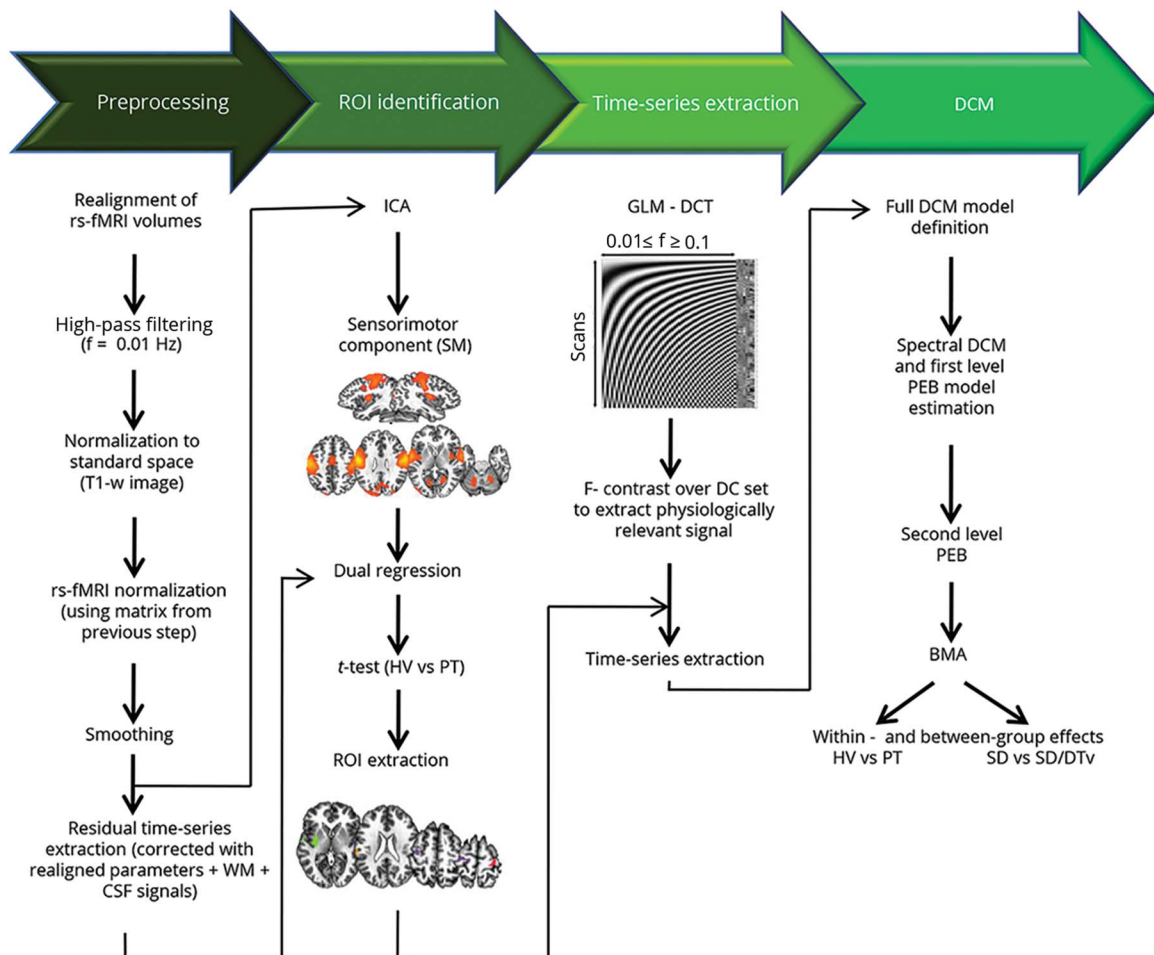
Functional connectivity: ICA

Preprocessed time series in all participants were concatenated and decomposed into spatial independent components with a temporal concatenation approach[14] in the Multivariate Exploratory Linear Optimized Decomposition Into Independent Components (MELODIC) toolbox of FSL software. The sensorimotor component was extracted because of its relevance to the pathophysiology of both SD and DTv.[15] Dual regression analysis[16,17] was run to evaluate between-group differences in functional coupling in the spatial component derived from the temporal concatenation ICA. This algorithm allowed identification of participant-specific temporal dynamics and associated temporal maps

for the component of interest. Each participant's residual 4-dimensional time series (after removal of 8 nuisance variables) were used as an input into the analysis. Voxel-based inferential statistics were run with a 2-sample t test on the individual z-value maps of the dual regression to compare functional connectivity between healthy controls and all patients. Statistical threshold was set at $p \leq 0.05$ after family-wise error correction for multiple comparisons over the component of interest. Significant clusters showing differences in functional connectivity between patients and controls were used as nodes on which the DCM was constructed.

GLM for time series extraction

Resting-state data were modeled with a GLM containing a discrete cosine basis set, consisting of 58 functions with frequencies characteristic of resting-state brain dynamics $(0.01–0.1 \text{ Hz})$[18,19] and the nuisance regressors that included 6 head motion parameters and WM and CSF signals. Mean time series over the regions identified in ICA were extracted

Figure 1 Analytical pipeline

Analytical pipeline of resting-state (rs) fMRI data processing for examination of functional and structural connectivity of the dystonic network. Data processing can be subdivided into 4 main steps, highlighted at the top. BMA = bayesian model averaging; DCM = dynamic causal modeling; DCT = discrete cosine transform; f = frequency; GLM = general linear model; HV = healthy volunteers; ICA = independent component analysis; PEB = parametric empirical Bayes; PT = patients; ROI = region of interest; SD = spasmodic dysphonia; SD/DTv = spasmodic dysphonia combined with dystonic tremor of voice; WM = white matter.

with the use of the principal eigenvariate adjusted for the confounding regressors. This was achieved by specifying an F contrast across the discrete cosine transforms to produce a statistical parametric map, which identified regions exhibiting blood oxygen level–dependent fluctuations within the frequency band. On quality checks, 5 healthy controls and 6 patients were excluded from DMC analysis because of insufficient time series extraction in 1 or more ROI. Thus, the final cohort of participants for effective connectivity analysis included 30 healthy controls and 34 patients (18 with SD and 16 with SD/DTv).

Effective connectivity: Spectral DCM with PEB

Typically, DCM analysis requires specification of a model space. Because there is no previous literature on resting-state regional influences within the dystonic network in SD, we adopted an approach that started with a fully connected model. This means that all 4 identified ROIs based on ICA between-group differences were connected to each other, generating a total of 16 connectivity parameters, including recurrent self-connections. We capitalized on the recent advances of modeling endogenous activity using spectral DCM in the framework of PEB[12] to inform the second-level group results (i.e., between-group effect). First, the full model was estimated and inverted for each participant with a hierarchical empirical bayesian inversion that alternated the estimation of DCMs at the first level (within participant) with the estimation of the group effect. At each iteration of the within-participant inversion, we updated the priors using empirical priors from the second level, which allowed us to draw participants out of local maxima. The bayesian model reduction[20] was applied after inversion of the full model.

After the first-level analysis, we created a second-level GLM that contained the parameters representing each within-participant and between-group effect on each DCM connection. We specified a design matrix with 2 regressors: 1 modeling the group mean and the second modeling the group differences. The algorithm optimized the empirical priors over the parameters of the set of first-level DCMs, using second-level constraints specified in the design matrix.

Finally, we performed bayesian model averaging of the second-level PEB model, describing the endogenous activity characteristic of resting-state fMRI data, to infer about connections best describing the mean group effect (all controls and all patients separately) and between-group differences (controls vs all patients and patients with SD vs patients with SD/DTv). The PEB framework permits never leaving the bayesian statistic, meaning that parameters have prior and posterior probability (PP) distributions and are described by their mean and covariance. As a result, parameters best describing within-group and between-group effects are reported not in terms of p value but instead in terms of PPs. PP values >0.8 were considered significant.

Data availability

Deidentified data and data analysis pipeline may be shared on request.

Results

Using ICA of resting-state fMRI data, we found decreased functional connectivity in the left putamen and inferior parietal cortex (IPC) as well as the bilateral premotor cortex (left, 2 clusters; right, 1 cluster) across all patients with SD and SD/DTv compared to healthy controls at family-wise error–corrected $p \leq 0.05$ (table 2 and figure 2A). This finding is in line with the previously reported deficits within the sensorimotor network in this disorder.[3,4,6–8,15,21,22] Thus, these regions were selected as nodes for DCM in the next step examining effective connectivity of the functional network. Two adjacent clusters in the left premotor cortex were merged into 1 region, resulting in a 4-node fully connected DCM configuration (figure 2B).
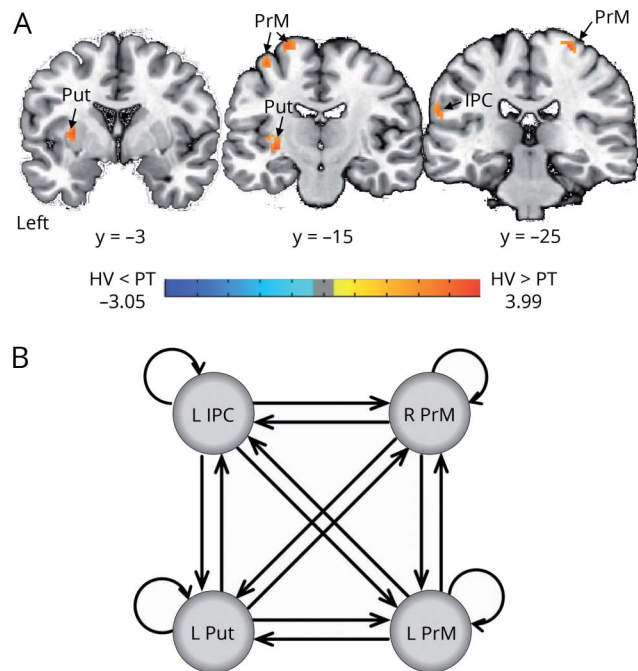
The unbiased, data-driven PEB algorithm identified 256 possible model configurations of a fully connected, 4-node network across all patients and healthy controls. Connection strengths from all models were averaged and weighted by their model evidence to derive bayesian model averaging. Across all patients and healthy controls, parameters best describing the combined group effect

Table 2 Significant clusters showing functional connectivity changes in all patients vs healthy controls as measured with ICA of resting-state fMRI data

Brain region	t Score	Coordinates xyz	Cluster size
Left putamen	3.99	−30, −14, −1	213
Left premotor cortex (area 6)	3.53	−22, −16, 67	64
Left premotor cortex (area 6)	3.50	−36, −16, 55	41
Left inferior parietal cortex (area PFop)	3.15	−58, −26, 21	45
Right premotor cortex (area 6)	3.62	24, −24, 63	41

Abbreviation: ICA = independent component analysis.

Figure 2 Identification of the brain regions used to build the DCM model

A

Put

PrM   PrM

Put   IPC

Left   y = −3   y = −15   y = −25

HV < PT   HV > PT
−3.05   3.99

B

L IPC   R PrM

L Put   L PrM

(A) Independent component analysis of resting-state fMRI data identified regional decreases in functional connectivity within the sensorimotor network between healthy controls (HVs) and patients (PT) with spasmodic dysphonia and dystonic tremor of voice at family-wise error–corrected $p \leq 0.05$. (B) These regions were used to construct the dynamic causal model (DCM). The fully connected model was built to estimate effective connectivity between the abnormal regions within the functional sensorimotor network. IPC = inferior parietal cortex; PrM = premotor cortex; Put = putamen.

included reciprocal excitatory influence of the left putamen onto bilateral premotor cortex and the left IPC onto bilateral premotor cortex and an excitatory directional influence from the left putamen to left IPC and from the left premotor cortex to its contralateral homolog. In addition, self-inhibitory connections were found in all 4 regions of the DCM network (all PPs = 1, figure 3A).

The excitatory directional connections from the left IPC to left putamen and from the right to left premotor cortices that showed no within-group effect (PP = 0) were instead the best discriminative parameters of between-group effect. Specifically, the excitatory influence of those directional connections was increased in a combined group of patients with SD and those with SD/DTv compared to healthy controls (PP = 1 for the connection from right to left premotor cortex, PP = 0.85 for the connection from left IPC to left putamen) (figure 3B).

In a direct comparison between the patient groups, decreased self-inhibitory influences in the left IPC and putamen as well as the right premotor cortex (all PPs = 0.83–0.99) modeled differences between patients with SD and those with SD/DTv (figure 3C).

Discussion

Examination of functional and effective connectivity between key regions of the sensorimotor network elucidated the mechanistic pattern underlying regional alterations in patients with SD with and without co-occurring DTv. There are 3 principal findings of this study. First, we confirmed and reproduced the presence of abnormally reduced functional connectivity within the sensorimotor network in this independent cohort of patients with focal dystonia and dystonic tremor compared to healthy controls. Second, we showed that hyperexcitable regional influences within the sensorimotor network are associated with their abnormal self-inhibitory function. Third, we demonstrated that disruption of the sensorimotor network in dystonia is both top-down, involving hyperexcitable parieto-putaminal connectivity, and interhemispheric, involving hyperexcitable premotor connectivity, both of which play an important role in processing of sensorimotor information in preparation for movement execution.

Sensorimotor brain regions examined for their functional and effective connectivity alterations in this study are well known in the literature to contribute to the pathophysiology of SD and other forms of dystonia.[4–6,8,23–26] It has been shown that premotor-parietal cortical areas and the putamen exhibit abnormally increased activity while patients are engaged in a task aimed at eliciting voice symptoms.[8,9,15] This is associated with abnormally increased putaminal dopamine release during symptomatic speech production[1] and abnormally decreased GABAergic function in the IPC.[27] These aberrations are further paralleled by decreased premotor-parietal and putaminal functional connectivity.[4,21,28] Vulnerable functional connectivity of premotor and inferior parietal regions, in particular, is linked to the polygenic risk of dystonia,[29] whereas abnormal putaminal connectivity underlies altered temporal discrimination, a mediational endophenotype of SD.[30] Although increased excitatory activity but decreased functional connectivity of the premotor-parietal-putaminal circuitry may seem at first a counterintuitive finding, it, in fact, reflects profound and complex disorganization of these brain regions and underscores their importance of forging and sustaining dystonic activity. Specifically, abnormal hyperexcitability of premotor-parietal-putaminal circuitry may be explained by altered information transfer between these regions during symptomatic task production due to underlying deficient connectivity. These alterations are present in patients with SD both with and without co-occurring dystonic tremor and are likely to be at the core of task-specific focal dystonia pathophysiology, or at least in the forms affecting the laryngeal muscles.

To that end, the similarity of neural circuit alterations in SD and DTv, in addition to previously reported shared functional and structural brain abnormalities,[15] once again suggests the presence of largely overlapping pathophysiology between these disorders. However, while hyperexcitable connectivity of the premotor-parietal cortex and putamen was

Figure 3 Results of the bayesian dynamic model comparison in HVs and patients with SD and SD/DTv
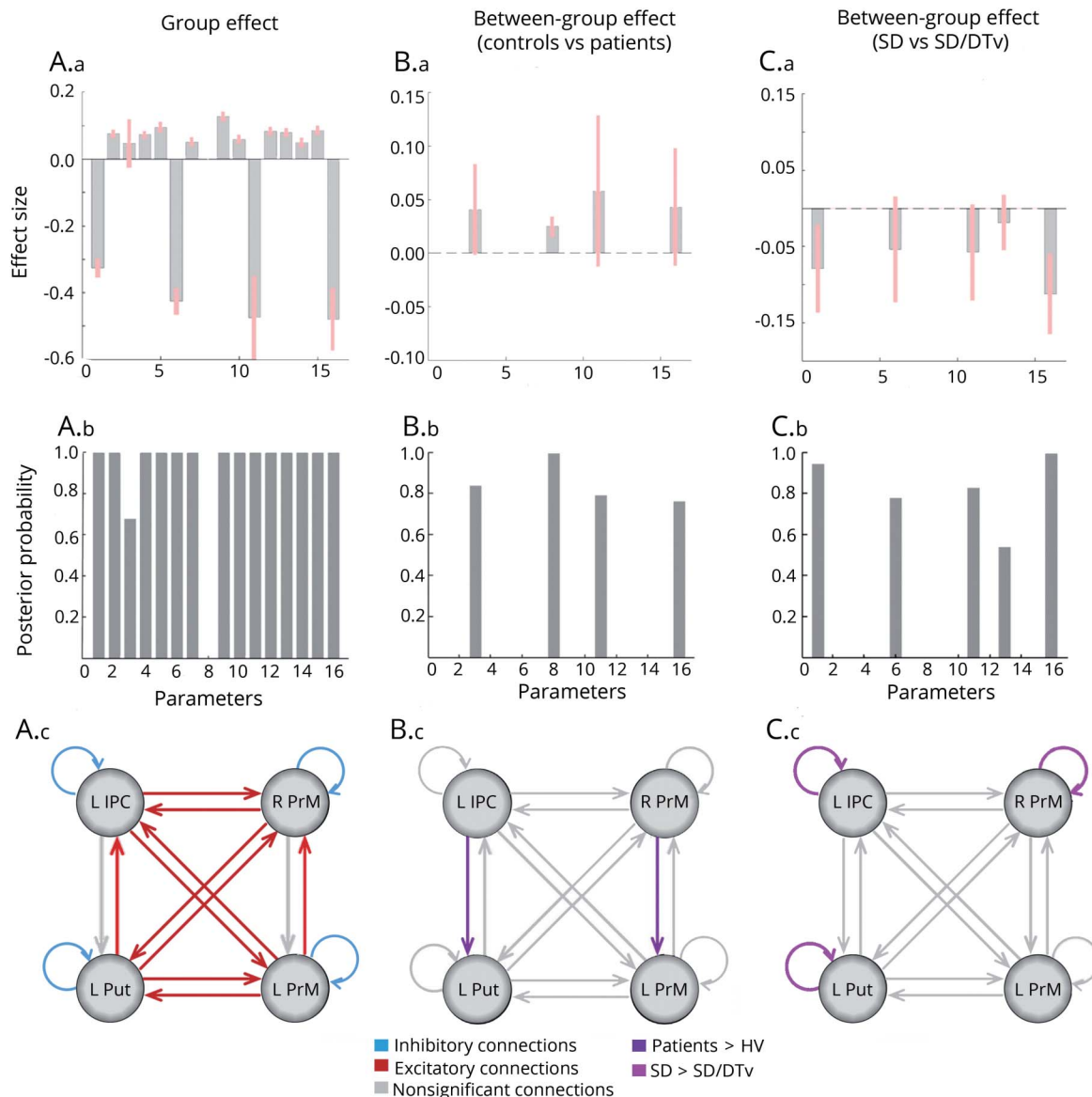
Panels A.a–A.c show the within-group effect for the effect size of each of the parameter in the model after bayesian model averaging (A.a), the corresponding posterior probabilities (PP; A.b), and a schematic representation of the significant excitatory connections (red), inhibitory connections (blue), and nonsignificant connections (gray). Panels B.a–B.c show the connections with strength that differed significantly between healthy controls and patients in terms of the effect size (B.a) and PPs (B.b). Panel B.c highlights between-group significant connections in purple and nonsignificant connections in gray. Panels C.a–C.c show connections with strength that differed significantly between patients with spasmodic dysphonia (SD) and those with SD/ dystonic tremor of voice (DTv) in terms of the effect size (C.a) and PPs (C.b). Panel C.c highlights between-group significant connections in purple and nonsignificant connections in gray. HV = healthy volunteers; IPC = inferior parietal cortex; PrM = premotor cortex; Put = putamen.

characteristic to both patient groups, differences existed in the magnitude of alterations involving regional recurrent self-inhibitory projections. In general, our finding of impaired inhibition is supported by the previous studies suggesting the presence of loss of inhibition as one of the hallmarks of dystonia pathophysiology.[31] It is important to note that loss of inhibition in the left IPC, right premotor cortex, and left putamen was greater in patients with combined SD and DTv than in those with SD only. A possible explanation for this may be the organization of the basal ganglia inhibitory circuitry and its contribution to the dystonia pathophysiology. It is known that putaminal medium spiny neurons (MSNs) receive an excitatory glutamatergic input from the cortex, while an inhibitory GABAergic input comes from the different sources, including MSN collaterals, pallidal feedback projections from globus pallidus, and feedforward projections from fast-spiking interneurons.[32–36] The fast-spiking interneurons control the spike timing of MSNs and balance cortical and thalamic excitation. A recent study in focal dystonia, including SD and SD/DTv patients, has shown that the physiologic balance between excitation and inhibition is impaired due to hyperfunctional direct basal ganglia pathway and hypofunctional indirect basal ganglia

pathway, collectively leading to abnormal thalamo-motocortical hyperexcitability.[2] Similarly, animal studies have shown that reduced putaminal feedforward inhibition produces paroxysmal dystonia in the dt^{sz} mutant hamster,[37] while selective inhibition of fast-spiking interneurons in rodents leads to dyskinesia, dystonia, and episodic tremor.[38,39] The manifested symptom variability was attributed to the differences between species and experimental and analytic protocols. Based on its symptomatology, frequency, and harmonics, an argument was made that selective inhibition of feedforward projections from fast-spiking interneurons leads to tremor rather than other types of movement disorders.[39] Characteristic to tremor, abnormal firing patterns of putaminal and pallidal neurons were temporarily and spatially correlated, becoming oscillatory and coherent with large-amplitude tremor.[39] Notably, selective reduction of the excitatory corticostriatal input resulted in the disappearance of tremor and the reversal of temporal and spatial correlatory activity. Such focal alterations of inhibition within the corticostriatal circuitry leading to or reversing tremor are supportive of our current finding of more prominent loss of inhibition in patients with SD with co-occurring DTv than SD alone.

In terms of abnormal information flow within the sensorimotor network, very little is known about the directionality of dystonic activity and causal inferences of one region on another. The only available study to date examined effective connectivity between the brain regions showing abnormal activity during finger tapping in patients with writer's cramp, another form of task-specific focal dystonia.[40] Although explicit alterations of regional functional connectivity within the examined circuitry were not mapped and the DCM regions were based on their activity only, this study found that the cerebellum established outgoing hyperexcitatory connections with the basal ganglia and primary motor cortex, whereas primary motocortical input/output projections with the basal ganglia appeared to be deficient. While these data provide evidence for the disrupted network organization that converges on the primary motor cortex as a final cortical output of dystonic movements, our findings, based on the stepwise evaluation of functional and effective connectivity of the sensorimotor cortex, rather show that the complex network disruption is staged well before the dystonic behavior is even produced by the primary motor cortex. This includes abnormally hyperexcitable top-down influences from the IPC to the putamen as well as abnormally hyperexcitable right-to-left interhemispheric influence on the premotor cortex. While the basal ganglia circuitry itself is profoundly abnormal in dystonia,[2] our current data suggest that it might be triggered by altered downstream cortico-putaminal projections. Another contributing factor may be abnormal connectivity of premotor cortex, which, together with the IPC, plays a critical role in sensorimotor processing and integration as preparatory stages to movement execution. Identification of bilateral premotor cortical involvement in the form of dystonia that predominantly affects speech production, a behavior that is thought to be dominant to the left hemisphere,[41] further points to a possible endophenotypic trait of this disorder that may contribute to the generation of the dystonic cascade.

Although numerous imaging studies have mapped brain abnormalities in dystonia, including SD, differentiation between primary causative and secondary compensatory changes remains unclear. Because our current findings provide evidence for alterations within the network that are driven by specific regions, it is conceivable that the identified pattern of abnormal parietal and premotor connectivity is causative rather than compensatory. Supportive of this assumption are several previous studies that found these regions to contribute to the polygenic risk of dystonia, correlate with SD symptom onset and subclinical abnormalities of sensory discrimination, play a critical role in large-scale functional network disorganization, and serve as potential neural biomarkers distinguishing between dystonic and healthy states.[4,21,28,30] Moreover, SD and DTv as disorders affecting a highly learned behavior, i.e., speech, require greater involvement of high-order cortical than subcortical regions.[22,42]

Taken together, our findings show that the complex disorganization of dystonic sensorimotor network activity is characterized by likely primary, top-down alteration of the balance between excitation and inhibition within the premotor-parietal-putaminal circuitry.

Appendix Authors

Name	Location	Role	Contribution
Giovanni Battistella, PhD	University of California San Francisco, California	Author	Acquisition of data; analysis of data; statistical analysis; drafting the manuscript
Kristina Simonyan, MD, PhD	Harvard Medical School, Boston, MA	Author	Study concept and design; acquisition of data; statistical analysis; commenting on the manuscript; study supervision; obtaining funding

References

1. Simonyan K, Berman BD, Herscovitch P, Hallett M. Abnormal striatal dopaminergic neurotransmission during rest and task production in spasmodic dysphonia. J Neurosci 2013;33:14705–14714.

2. Simonyan K, Cho H, Hamzehei Sichani A, Rubien-Thomas E, Hallett M. The direct basal ganglia pathway is hyperfunctional in focal dystonia. Brain 2017;140:3179–3190.

3. Ali SO, Thomassen M, Schulz GM, et al. Alterations in CNS activity induced by botulinum toxin treatment in spasmodic dysphonia: an H215O PET study. J Speech Lang Hear Res 2006;49:1127–1146.

4. Battistella G, Fuertinger S, Fleysher L, Ozelius LJ, Simonyan K. Cortical sensorimotor alterations classify clinical phenotype and putative genotype of spasmodic dysphonia. Eur J Neurol 2016;23:1517–1527.

5. Battistella G, Termsarasab P, Ramdhani RA, Fuertinger S, Simonyan K. Isolated focal dystonia as a disorder of large-scale functional networks. Cereb Cortex 2017;27:1203–1215.

6. Haslinger B, Erhard P, Dresel C, Castrop F, Roettinger M, Ceballos-Baumann AO. Silent event-related fMRI reveals reduced sensorimotor activation in laryngeal dystonia. Neurology 2005;65:1562–1569.

7. Kostic VS, Agosta F, Sarro L, et al. Brain structural changes in spasmodic dysphonia: a multimodal magnetic resonance imaging study. Parkinsonism Relat Disord 2016;25:78–84.

8. Simonyan K, Ludlow CL. Abnormal activation of the primary somatosensory cortex in spasmodic dysphonia: an fMRI study. Cereb Cortex 2010;20:2749–2759.

9. Simonyan K, Ludlow CL. Abnormal structure-function relationship in spasmodic dysphonia. Cereb Cortex 2012;22:417–425.

10. Simonyan K, Tovar-Moll F, Ostuni J, et al. Focal white matter changes in spasmodic dysphonia: a combined diffusion tensor imaging and neuropathological study. Brain 2008;131:447–459.

11. Baltusis L, Gu M, Hurd RE, et al. Editing with MEGA-PRESS and MEGA-SPECIAL-PD Sequences. Presented at the Experimental NMR Conference (ENC); April 10–15, 2016; Pittsburgh.

12. Friston KJ, Litvak V, Oswal A, et al. Bayesian model reduction and empirical Bayes for group (DCM) studies. Neuroimage 2016;128:413–431.

13. Ashburner J, Friston KJ. Unified segmentation. Neuroimage 2005;26:839–851.

14. Beckmann CF, DeLuca M, Devlin JT, Smith SM. Investigations into resting-state connectivity using independent component analysis. Philos Trans R Soc Lond B Biol Sci 2005;360:1001–1013.

15. Kirke DN, Battistella G, Kumar V, et al. Neural correlates of dystonic tremor: a multimodal study of voice tremor in spasmodic dysphonia. Brain Imaging Behav 2017;11:166–175.

16. Filippini N, MacIntosh BJ, Hough MG, et al. Distinct patterns of brain activity in young carriers of the APOE-epsilon4 allele. Proc Natl Acad Sci USA 2009;106:7209–7214.

17. Leech R, Kamourieh S, Beckmann CF, Sharp DJ. Fractionating the default mode network: distinct contributions of the ventral and dorsal posterior cingulate cortex to cognitive control. J Neurosci 2011;31:3217–3224.

18. Fransson P. Spontaneous low-frequency BOLD signal fluctuations: an fMRI investigation of the resting-state default mode of brain function hypothesis. Hum Brain Mapp 2005;26:15–29.

19. Kahan J, Urner M, Moran R, et al. Resting state functional MRI in Parkinson's disease: the impact of deep brain stimulation on "effective" connectivity. Brain 2014;137:1130–1144.

20. Friston K, Penny W. Post hoc bayesian model selection. Neuroimage 2011;56:2089–2099.

21. Putzel GG, Battistella G, Rumbach AF, Ozelius LJ, Sabuncu MR, Simonyan K. Polygenic risk of spasmodic dysphonia is associated with vulnerable sensorimotor connectivity. Cereb Cortex 2018;28:158–166.

22. Battistella G, Termsarasab P, Ramdhani RA, Fuertinger S, Simonyan K. Isolated focal dystonia as a disorder of large-scale functional networks. Cereb Cortex 2017;27:1203–1215.

23. Delnooz CC, Pasman JW, Beckmann CF, van de Warrenburg BP. Task-free functional MRI in cervical dystonia reveals multi-network changes that partially normalize with botulinum toxin. PLoS One 2013;8:e62877.

24. Løkkegaard A, Herz DM, Haagensen BN, Lorentzen AK, Eickhoff SB, Siebner HR. Altered sensorimotor activation patterns in idiopathic dystonia-an activation likelihood estimation meta-analysis of functional brain imaging studies. Hum Brain Mapp 2016;37:547–557.

25. Gallea C, Horovitz SG, Ali Najee-Ullah M, Hallett M. Impairment of a parieto-premotor network specialized for handwriting in writer's cramp. Hum Brain Mapp 2016;37:4363–4375.

26. Porcacchia P, Palomar FJ, Caceres-Redondo MT, et al. Parieto-motor cortical dysfunction in primary cervical dystonia. Brain stimulation 2014;7:650–657.

27. Simonyan K. Inferior parietal cortex as a hub of loss of inhibition and maladaptive plasticity. Presented at the Annual Meeting of American Academy of Neurology; April 22–28, 2017; Boston.

28. Fuertinger S, Simonyan K. Connectome-wide phenotypical and genotypical associations in focal dystonia. J Neurosci 2017;37:7438–7449.

29. Putzel GG, Fuchs T, Battistella G, et al. GNAL mutation in isolated laryngeal dystonia. Mov Disord 2016;31:750–755.

30. Termsarasab P, Ramdhani RA, Battistella G, et al. Neural correlates of abnormal sensory discrimination in laryngeal dystonia. Neuroimage Clin 2016;10:18–26.

31. Hallett M. Neurophysiology of dystonia: the role of inhibition. Neurobiol Dis 2011;42:177–184.

32. Tunstall MJ, Oorschot DE, Kean A, Wickens JR. Inhibitory interactions between spiny projection neurons in the rat striatum. J Neurophysiol 2002;88:1263–1269.

33. Mallet N, Micklem BR, Henny P, et al. Dichotomous organization of the external globus pallidus. Neuron 2012;74:1075–1086.

34. Koós T, Tepper JM. Inhibitory control of neostriatal projection neurons by GABAergic interneurons. Nat Neurosci 1999;2:467–472.

35. Berke JD. Functional properties of striatal fast-spiking interneurons. Front Syst Neurosci 2011;5:45.

36. Parthasarathy HB, Graybiel AM. Cortically driven immediate-early gene expression reflects modular influence of sensorimotor cortex on identified striatal neurons in the squirrel monkey. J Neurosci 1997;17:2477–2491.

37. Gernert M, Hamann M, Bennay M, Loscher W, Richter A. Deficit of striatal parvalbumin-reactive GABAergic interneurons and decreased basal ganglia output in a genetic rodent model of idiopathic paroxysmal dystonia. J Neurosci 2000;20:7052–7058.

38. Gittis AH, Leventhal DK, Fensterheim BA, Pettibone JR, Berke JD, Kreitzer AC. Selective inhibition of striatal fast-spiking interneurons causes dyskinesias. J Neurosci 2011;31:15727–15731.

39. Oran Y, Bar-Gad I. Loss of balance between striatal feedforward inhibition and corticostriatal excitation leads to tremor. J Neurosci 2018;38:1699–1710.

40. Rothkirch I, Granert O, Knutzen A, et al. Dynamic causal modeling revealed dysfunctional effective connectivity in both, the cortico-basal-ganglia and the cerebello-cortical motor network in writers' cramp. Neuroimage Clin 2018;18:149–159.

41. Price CJ. The anatomy of language: contributions from functional neuroimaging. J Anat 2000;197(pt 3):335–359.

42. Ramdhani RA, Kumar V, Velickovic M, Frucht SJ, Tagliati M, Simonyan K. What's special about task in dystonia? A voxel-based morphometry and diffusion weighted imaging study. Mov Disord 2014;29:1141–1150.